

Synthesis, Characterization, Evolution of Potential application of Ce metal complexes as luminescent markers for explosives 1, 2, 4, 5-benzenetetracarboxylic acid

Zarmeen Saleem¹, Muhammad Farhan^{2*}, Hafsa Irum³, Warda Shaz², Hafiz Muhammad Kashif Zahoor⁴, Asfoora Azmat⁵

¹Department of Chemistry, Government College University Lahore, Punjab, Pakistan

²Institute of Molecular Biology and Biotechnology, Department of Forensic Science, The University of Lahore, Lahore, Pakistan

³Institute of Molecular Biology and Biotechnology, Department of Microbiology, The University of Lahore, Lahore, Pakistan

⁴Institute of Chemistry, The Islamia University of Bahawalpur, Punjab, Pakistan

⁵Sahara Medical College Narowal, Punjab, Pakistan

Received: 23 October, 2025, Revised: 15 December, 2025, Accepted: 17 December, 2025, online: 17 December 2025

© The Author(s) 2024

Abstract

The development of rapid, selective, and sensitive detection methods for nitroaromatic explosives is critically important for forensic science and security applications. In this study, two cerium-based metal–organic complexes were synthesized via a sonication-assisted method using 1,2,4,5-benzenetetracarboxylic acid as the primary ligand, both in the absence and presence of the co-ligand 2-[(hydroxy-2-methyl-5-phosphonoxymethyl-pyridin-4-ylmethyl)amino]-propionic acid. The synthesized complexes were characterized by Fourier-transform infrared spectroscopy, ultraviolet–visible spectroscopy, and photoluminescence spectroscopy. Fluorescence sensing experiments revealed that both complexes exhibit high selectivity and sensitivity toward picric acid (2,4,6-trinitrophenol) among a range of nitroaromatic analytes. Notably, the co-ligand-containing complex demonstrated enhanced fluorescence quenching efficiency and larger Stern–Volmer constants. These findings highlight the potential of cerium complexes based on 1,2,4,5-benzenetetracarboxylic acid as effective luminescent probes for the identification of explosive compounds, enabling rapid and safe detection of hazardous materials in security-related scenarios and forensic investigations.

Keywords Cerium complexes, Luminescent sensor, Nitroaromatic explosives, Picric acid, Fluorescence quenching,

✉ 1st Author zarmeench27@gmail.com

✉ 2nd Author kkfarhan004@gmail.com

✉ 3rd Author hafsahirum@outlook.com

✉ 4th Author wardafjwu@gmail.com

✉ 5th Authors kashifzahoor95@gmail.com

✉ corresponding kkfarhan004@gmail.com

Published Online 17 December 2025

Crossref: doi.xxxxxxxxxx pending

ISSN: 000-0000 Pending

1. Introduction

Coordination polymers are a type of organometallic or inorganic material consisting of metal ions or clusters which are linked to

organic ligands by coordinate covalent bonds. Such structures may be one, two or three dimensional, resulting in networks with a variety of architectures and properties. The coordination of the ligands with the metal centers are completed through the donation of electron pairs where the ligands are Lewis bases and the metal centers are Lewis's acids. Based on the number of donor atoms they contribute to the binding of metals; ligands could either be monodentate or polydentate with respect to the coordination properties. The range of color in transition metal-based coordination complexes is one of their more notable characteristics and is due to d-d transitions within metal ions with partially filled d orbitals (generally d 2 -d 9 in composition) (Zhou & Frenking, 2021).

In the last several decades, coordination polymers have attracted more attention of scientists because of their exotic structural diversity and perspectives in multiple fields, such as

photoluminescence, catalysis, magnetism, sorption of gases, drug delivery, or explosives detection (Wang et al., 2020). Nonetheless, the design and synthesis of new functional coordination polymers can be problematic because numerous parameters are also involved such as nature of metal ions, ligand geometry, solvent systems, reaction pH, and temperature (Roy et al., 2016). Ligand selection is one of such factors, which is particularly important. Even though the synthesis of a single liganded polymer might be quite easy, numerous researchers are inclined to utilize multiple ligands to attain the desired functionality and a greater storage of structural complexity (Ding et al., 2023).

The remarkable ability to fluorescence and explosives sensing in coordination polymers especially those that make metal-organic frameworks (MOFs) has also been reported (Cui et al., 2023). Their contribution in the area of forensic science is gaining prominence. In cases such as sexual assault, hit-and-run incidents, arson, and armed robbery, MOFs have demonstrated potential in detecting trace evidences like gunshot residues (GSR) and cosmetic traces. For example, metal complexes in MOFs can detect residues from lipsticks, perfumes, eyeliners, nail polish, and other personal care products, which often transfer to clothing, drinking utensils, cigarette butts, or tissues at crime scenes. These residues, when recovered, can indicate direct physical contact between victims and perpetrators, offering crucial forensic links (Abdi & Sarlak, 2025).

MOFs represent a relatively new and growing class of crystalline, porous coordination networks that possess a wide range of applications in chemistry, biochemistry, industrial chemistry, and materials science. Constructed from metal ions or clusters (acting as nodes) bridged by multidentate organic ligands (acting as linkers), MOFs can exist in one-dimensional (1D), two-dimensional (2D), or three-dimensional (3D) structures. Their ultra-high porosity and extensive surface area offer advantages over traditional porous materials like zeolites. Microporous MOFs have pore diameters under 2 nm, while mesoporous types range between 2–50 nm, allowing for selective guest molecule interactions (Guo et al., 2022).

Over the last three decades, the scientific community has recognized the vast potential of MOFs. Their applications span water purification, electrochemical sensors, heterogeneous catalysis, drug delivery, and biomedical imaging. In catalysis, MOFs offer fast, cost-effective reaction pathways, provided the reaction environment pH, solvent type, and temperature is properly optimized (Socha et al., 2024). In biomedical

applications, MOFs are being investigated for drug encapsulation and targeted release, although the concern of potential toxicity remains. Nevertheless, the controlled release capabilities of MOFs are promising for therapeutic monitoring (Chen et al., 2022).

One emerging and impactful application of MOFs lies in the field of explosive detection. Luminescent MOFs and coordination complexes particularly those containing lanthanide ions are being explored as chemical markers in ammunition and explosives. These luminescent markers provide unique optical fingerprints, which can assist in tracking the source of ammunition and enhance gunshot residue detection (Sun et al., 2023). The incorporation of lanthanides like cerium in coordination polymers not only enhances luminescent performance but also offers chemical stability and structural versatility.

Cerium-based metal-organic frameworks (Ce-MOFs) are especially promising in the detection of nitroaromatic explosives such as TNT, DNT, and picric acid. Cerium, a rare-earth element, exhibits useful optical and redox properties due to its Ce^{3+}/Ce^{4+} redox couple. However, while Ce^{3+} complexes are known for their strong luminescence, a known limitation is their potential toxicity upon prolonged exposure, which must be considered in biomedical or environmental applications (D. Zhao et al., 2022).

In this study, the organic ligand of interest is 1,2,4,5-benzenetetracarboxylic acid (H_4BTCA), a tetra carboxylate compound capable of forming multiple coordination sites with metal ions. Its symmetrical structure and electron-rich nature make it suitable for constructing luminescent coordination networks. By coordinating H_4BTCA with cerium ions, novel Ce-based coordination complexes can be synthesized with potential use as luminescent markers for explosives detection. However, to verify the successful synthesis and investigate their functional properties, several characterizations i.e. Ultraviolet–visible (UV–Vis) spectroscopy Fourier-transform infrared (FTIR) spectroscopy and Photoluminescence (PL) spectroscopy were used. Together, these techniques UV-Vis, FTIR, and PL-offer comprehensive insight into the structural and photophysical characteristics of Ce– H_4BTCA coordination complexes. Through the synthesis of these materials and by determining their behavior in relation to luminescence quenching in the presence of the nitroaromatic explosives, this paper therefore seeks to provide an additional and cost-effective selective method of detecting explosives. These materials could be used in portable detection

platforms, security screening and forensic science applications where a fast reliable identification of explosives is essential.

2. Materials and Methods

2.1. Materials

Synthesis and characterization of the cerium metal complexes utilized different chemicals, solvents, apparatus used in a laboratory and instrumentations. The principal reagents were: 1,2,4,5-benzenetetracarboxylic acid, cerium nitrate hexahydrate and a co-ligand a: 2-[(hydroxyl-2-methyl-5-phosphonoxymethyl-pyridine-4-ymethyl)-amino]-propionic acid (PDA). The reaction steps and purification processes as well employed the use of organic reagents in the form of ethanol, methanol, n-hexane, diethylformamide (DMF), acetonitrile (ACN) and 1,4-dioxane. Synthesis and solution preparations were also done using sodium nitrate and distilled water. Basic laboratory glassware and accessories involved vials, aluminum flasks, excellent plates, sonicator, spatula, measuring tools, Eppendorf droppers, beakers, filters, pipette, pipette suckers, filter paper, measuring cylinders, and confections, reagent bottles, tripod stands, UV lamps and thermometers.

Besides the core materials, other miscellaneous materials that were needed to facilitate the lab work were the paper tape, markers, pH paper, covering fundamental lids, and scissors. To validate the sensing characteristics of the synthesized luminescent markers, a number of explosive compounds were tested among which were picric acid (2,4,6-trinitrophenol), nitroaniline (4-NA), 4-nitrophenol (4-NP), and 4-nitrotoluene (4-NT). Microsoft Word 2020, PowerPoint 2020, Excel 2020, and Origin software were utilized as software tools during the research to assist in the analysis and the structural drawing process.

Instrumentation played a crucial role in both the synthesis and characterization phases. The main instruments utilized included an electronic weighing balance for accurate measurement of reagents, a UV-visible spectrophotometer for absorption studies, a sonicator for homogeneous mixing and dispersion of reactants, a microscope for morphological observations, and a fluorescence spectrophotometer for photoluminescence measurements of the synthesized complexes.

2.2 Synthesis of Metal Complexes

Complex 1 was synthesized using a sonochemical approach. Initially, a solution of cerium nitrate (0.2 mmol, 86 mg) was prepared in 2 mL of distilled water, while a separate solution of 1,2,4,5-benzenetetracarboxylic acid (0.4 mmol, 100 mg) was

dissolved in 4 mL of distilled water. The pH of both solutions was checked prior to mixing. The cerium salt solution was subjected to sonication for 5 minutes to ensure complete dissolution and uniform dispersion. If necessary, the ligand solution was sonicated for an additional 1 minute. After preparation, both solutions were combined in a single vial and sonicated together for 15 to 20 minutes to facilitate coordination and complex formation. The final reaction mixture was left undisturbed in the air to dry at room temperature for a period of 15 to 20 days. After this duration, rod-like, colorless crystals of the complex were successfully obtained.

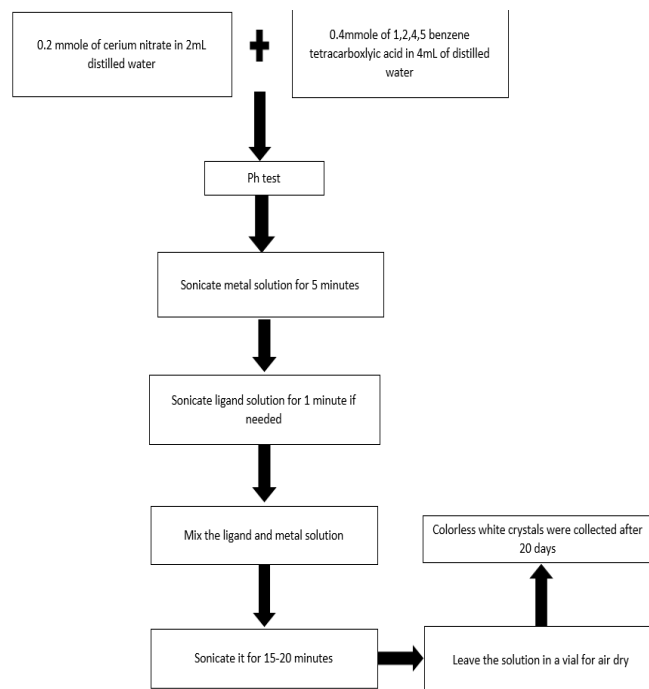


Figure 1. Synthesis scheme of complex 1

2.3 Method for Complex 2

Complex 2 was also synthesized using the sonication method. In a single vial, 0.2 mmol (86 mg) of cerium nitrate, 0.4 mmol (100 mg) of 1,2,4,5-benzenetetracarboxylic acid, and 0.2 mmol (19.9 mg) of PPDA were combined. In a separate vial, a solvent mixture containing 2 mL of ethanol and 4 mL of distilled water was prepared. The cerium salt, primary ligand, and co-ligand were then added to the solvent mixture. Sonication was performed with the total solution of 5 to 10 minutes to facilitate complex formation. The air-drying process was then carried out by allowing sonication vial to rest at room temperature without disturbing it until 15 to 20 days. At 20 days, complex 2 formed colored, sharp-needle-like crystals.

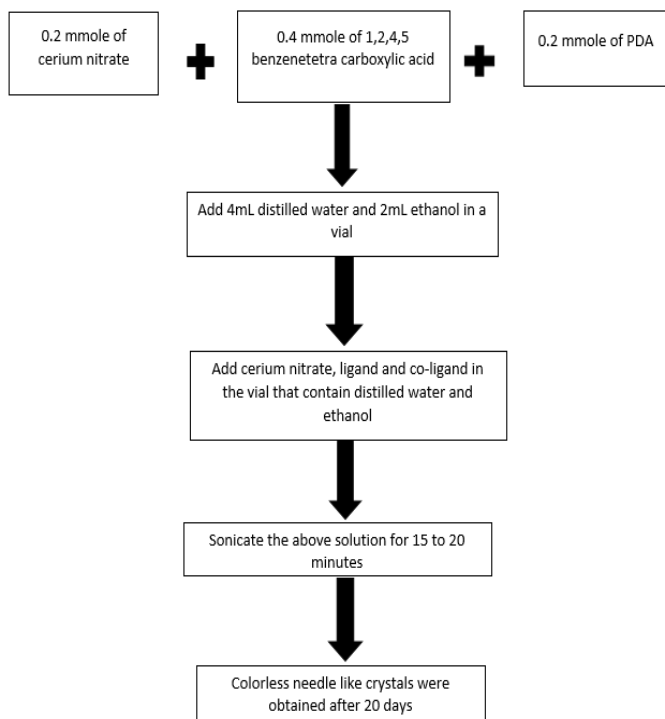


Figure 2. Synthesis scheme of complex 2

2.4 Characterization of metal complexes

A number of spectroscopic methods were used to characterize the synthesized metal complexes. The functional groups in the complexes were characterized by FTIR spectroscopy, which lead to the determination of the molecular structures. UV-visible spectroscopy was applied to the demonstration of the successful ligation and association of the metal ion with the organic ligand. Further, to determine the luminescent characteristics of the complexes, photoluminescence analysis was performed. The method was also used to understand the aspects of sensitivity of the complexes to nitroaromatic compounds that form major components in most explosive materials.

2.5 Nitro aromatic compounds explosives sensing

Step 1:

The sensitivity of the synthesized complexes to nitroaromatic explosive products was tested in two major steps. During the first step, solutions of Complex 1 and 2 were prepared using various solvents. To this end, 1 mg of both complexes were individually dissolved in several solvents such as methanol, 1,4-dioxane, n-hexane, acetonitrile, and butanol. Excitation and emission wavelengths of the complexes were measured in all the solvents and compared to evaluate the solvent that best suited the sensing research employing fluorescence.

Step 2:

The second step involved preparation of different solutions of varied concentrations of other nitroaromatic compounds within explosives such as 2,4,6-trinitrophenol (picric acid), 4-nitroaniline (4-NA), 4-nitrophenol (4-NP), and 4-nitrotoluene (4-NT) to examine their quenching effect. The metal complexes showed different photoluminescence behavior with all these nitro compounds. To evaluate the quenching behavior, a graph was plotted between the concentration of the nitro compounds and the fluorescence intensity ratio (I/I_0). The slope, intercept, and R^2 values were then calculated based on the data obtained from the photoluminescence measurements. components in most explosive materials.

3. Results and Discussion

3.1 Physical properties of the complexes:

The physical properties of the synthesized complexes, including their color, shape, size, and solubility in various solvents, were carefully observed. Complex 1 appeared colorless with a distinct rod-shaped crystalline structure, as shown in Figure 4.1 under microscopic examination. Similarly, Complex 2 also exhibited a colorless appearance but with a needle-like crystalline form, as illustrated in Figure 4.2. These physical characteristics helped in confirming the successful formation and morphology of the metal complexes.



Figure 3. Microscopic picture of Complex 1

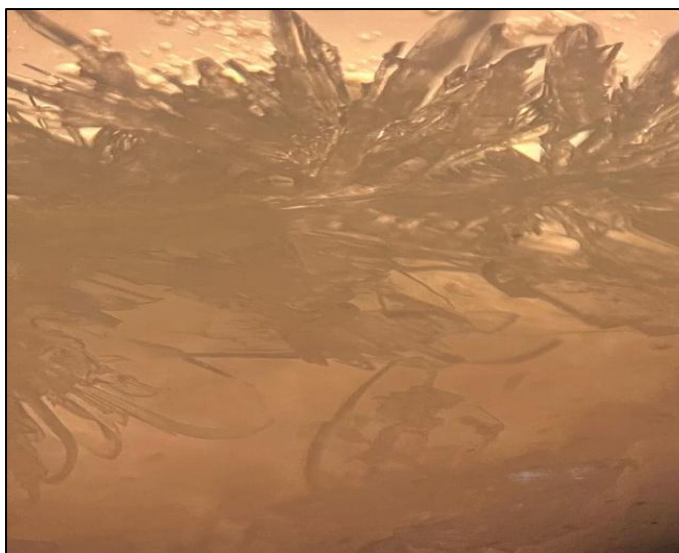


Figure 4. Microscopic picture of complex 2

3.2 Solubility of the complexes:

Solubility of the complex 1 and 2 were find by dissolving both complexes in different solvents as shown in table 1.

Table 1: solubility of complexes in different solvents.

Complexes	Distilled water	Methanol	Ethanol	1,4-dioxane	Acetonitrile	DMF
1	Soluble	Partially soluble	Partially soluble	Partially soluble	Soluble	Partially soluble
2	Soluble	Partially soluble	Partially soluble	Soluble	Soluble	Partially soluble

3.3 FTIR Analysis of the complexes:

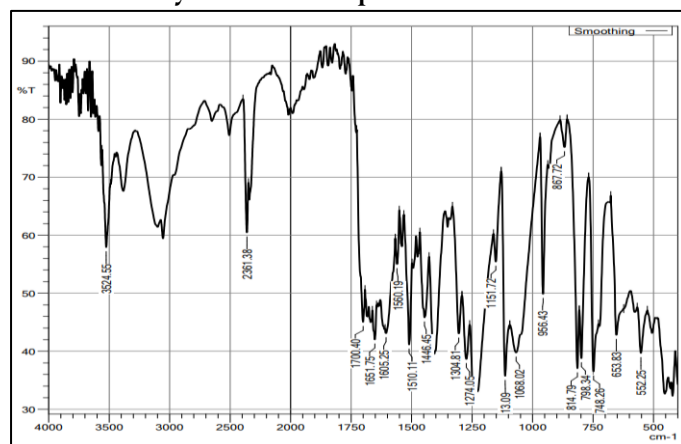


Figure 5. FT-IR spectrum of the complex 1

The FT-IR spectrum of Complex 1 was recorded within the range of 4000–500 cm^{-1} . A broad band corresponding to the

stretching vibration of the hydroxyl group (VOH) was observed to shift from its original position at 3854 cm^{-1} to 2381.38 cm^{-1} , indicating successful complex formation. Additionally, a series of smaller peaks ranging from 1700.40 cm^{-1} to 1151.1 cm^{-1} further confirmed complexation, likely due to the involvement of hydroxyl groups from water molecules and carboxyl groups from the ligand. Furthermore, the presence of bands in the fingerprint region between 653.8 cm^{-1} and 552.25 cm^{-1} confirmed the formation of metal-oxygen (M–O) bonds, supporting the successful coordination of the metal ion with the ligand.

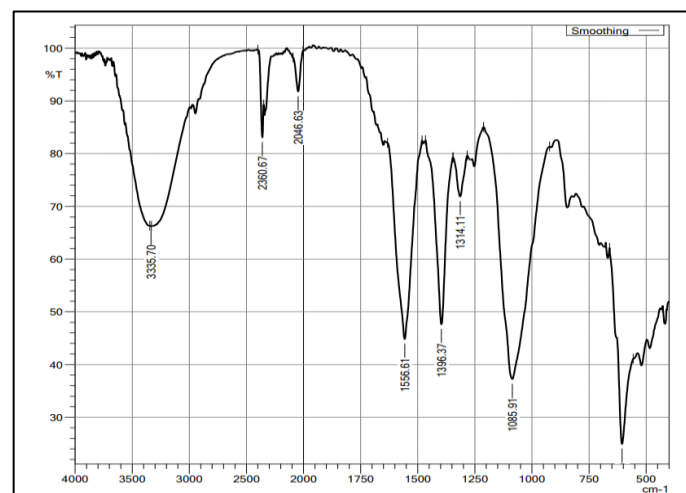


Figure 6. FT-IR spectrum of the complex 2

The FT-IR Spectrum of Complex 2 was measured between 4000–500 cm^{-1} . One of the large peaks at 3335.7 cm^{-1} was attributed to the presence of the water (H_2O) used under the solvent. The formation of carbonyl group was indicated by a medium-intensity peak at 1556.61 cm^{-1} , a portion of the complex affirmed by the formation of the bond. Another peak about 1396.37 cm^{-1} was linked to the aromatic rings in the compound which further authenticated the structural properties of the compound.

3.4 Comparison between the peaks and bands in pure ligand and complexes

The observation of the FT-IR spectral data of the pure ligand in comparison with complexes synthesized shows that there are high structural variations that affirm the formation of complex. In the ligand, a sharp peak was observed at 1118 cm^{-1} , which shifted to 1510.1 cm^{-1} in Complex 1 and 1085.95 cm^{-1} in Complex 2, indicating changes in the bonding environment. A broad peak originally present at 3145 cm^{-1} in the ligand disappeared in Complex 1 but was observed at 3335.70 cm^{-1} in Complex 2, likely due to the presence of solvent (H_2O). The small peaks

ranging from 1278 to 1614 cm^{-1} in the ligand were shifted to 1304.81–1651 cm^{-1} in Complex 1 and 1314.11–1556.1 cm^{-1} in Complex 2, which supports modifications in the functional groups involved in coordination. Additionally, a peak at 2649 cm^{-1} was found in the ligand within the 2500–3500 cm^{-1} range. The OH stretching peak was clearly observed at 3524.45 cm^{-1} in the ligand but was absent in Complex 2, suggesting hydrogen bonding interactions or involvement in coordination. A new peak around 2361.38 cm^{-1} appeared in both complexes but was not present in the ligand, providing further evidence for the successful formation of metal–ligand coordination complexes.

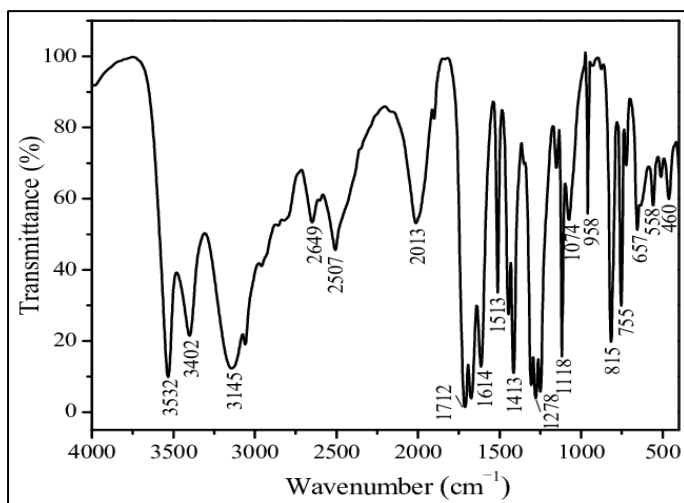


Figure 7. IR spectrum of pure ligand

Table 2: shows the difference in the structure of ligand before and after the complex formation.

Peaks and Bands	Ligand	Compl ex 1	Compl ex 2
Sharp peak	1118 cm^{-1}	1510.1 cm^{-1}	1085.95 cm^{-1}
Broad peak	3145 cm^{-1}	no	3335.70 cm^{-1}
Small peaks	1278-1614 cm^{-1}	1304.81-1651 cm^{-1}	1314.11-1556.1 cm^{-1}
Peaks at 2500 - 3500	2649 cm^{-1} OH, stretching peak	3524.45 cm^{-1} OH, stretching peak	no
Peak at 2361.38	no	yes	yes

3.5 UV visible spectroscopy of Complex 1

To investigate the optical properties of Complex 1, a UV-visible spectroscopic analysis was performed. A solution was prepared by dissolving 1 mg of Complex 1 in 5 mL of methanol, followed by sonication for 10 minutes to obtain a clear solution. The absorbance spectrum was recorded in the range of 200–800 nm using a UV-visible spectrometer. The maximum absorption wavelength (λ_{max}) for Complex 1 was observed at 285 nm with an absorbance of 3.8, which lies in the ultraviolet (UV) region and is attributed to π – π^* electronic transitions.

In comparison, the λ_{max} of the free ligand was recorded at 255 nm. The observed blue shift in the absorption band of Complex 1 relative to the ligand indicates a decrease in conjugation upon coordination with the metal center. This decrease in conjugation increases the energy gap between the π – π^* transitions, leading to the observed shift toward a shorter wavelength. The blue shift thus confirms that metal coordination weakens the conjugated system of the ligand, supporting successful complex formation.

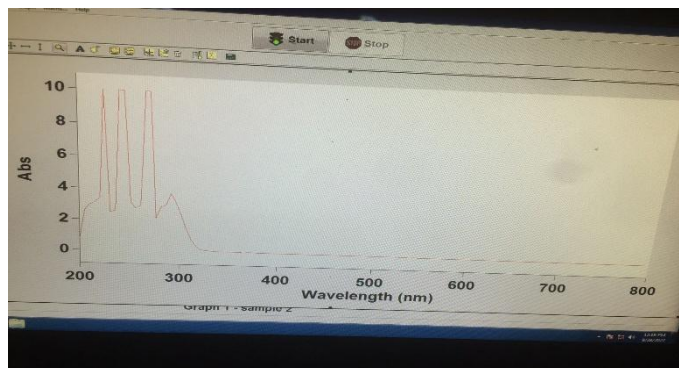


Figure 8. UV visible spectra of complex 1

3.6 UV visible spectroscopy of complex 2

To analyze the optical properties of Complex 2, a UV-visible spectroscopic study was conducted. A solution was prepared by dissolving 1 mg of Complex 2 in 5 mL of methanol, followed by sonication for 10 minutes to ensure complete dissolution and clarity of the solution. The UV-visible spectrum was recorded within the wavelength range of 200–800 nm. The maximum absorption wavelength (λ_{max}) for Complex 2 was observed at 290 nm with an absorbance value of 2.2. This λ_{max} lies in the ultraviolet (UV) region and is attributed to π – π^* electronic transitions.

For comparison, the λ_{max} values of the free ligand and co-ligand were observed at 255 nm and 240 nm, respectively. The absorption band of Complex 2 shows a blue shift compared to both ligands, indicating a reduction in the conjugation system

upon metal coordination. This decrease in conjugation results in an increased energy gap for $\pi-\pi^*$ transitions. Consequently, the observed blue shift supports the conclusion that the conjugated system of the ligand has been weakened after complex formation with the metal ion.

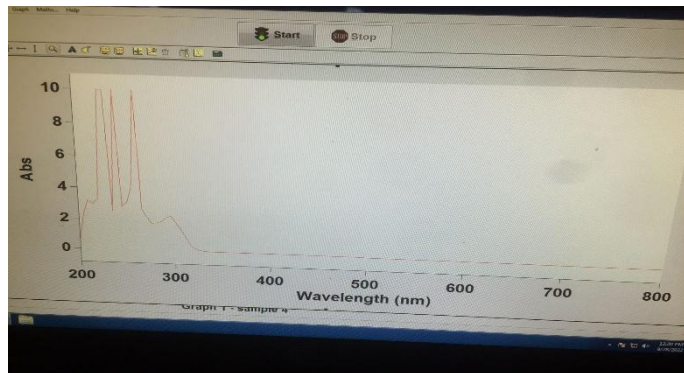


Figure 9. UV visible spectra of complex 2

3.7 Nitroaromatics Explosives Sensing

To determine the optimal solvent for explosive sensing applications, 1 mg of Complex 1 was dispersed separately in methanol, 1,4-dioxane, distilled water, acetonitrile (ACN), and n-hexane. In each case, partial solubility was observed, and the dispersions were stabilized through 10 minutes of bath sonication. The fluorescence spectra for each dispersion were then recorded. Among the tested solvents, methanol exhibited the highest fluorescence emission intensity, whereas distilled water showed the lowest response. This clearly indicates methanol as the most suitable solvent for dispersing Complex 1, offering both strong luminescence and good stability. When excited at 312.03 nm in methanol, the complex exhibited a strong emission peak at 783.84 nm (Figure 4.8 and Figure 4.9), highlighting its potential as an efficient luminescent probe for nitroaromatic explosive detection.

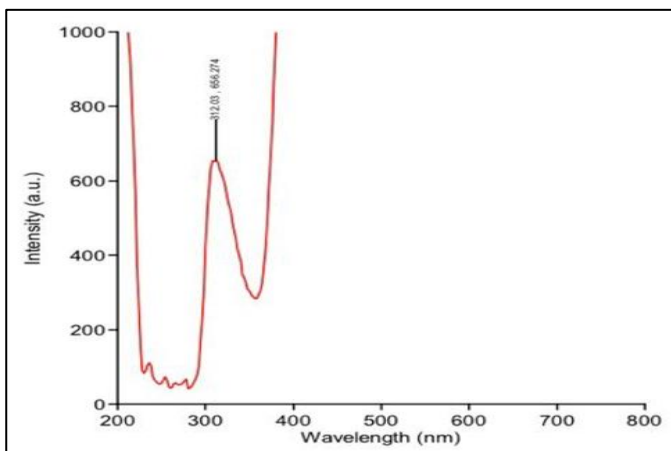


Figure 10. Excitation peak of complex 1

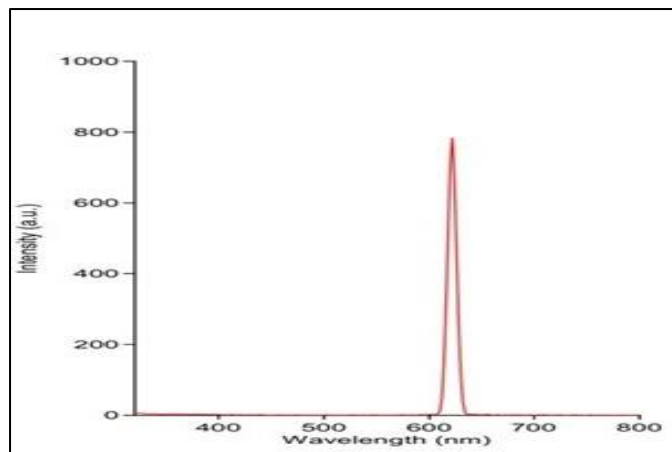


Figure 11. Emission peak of complex 1

The higher fluorescence in methanol can be attributed to its polar protic nature, which promotes strong solute–solvent interactions and suppresses non-radiative decay pathways. Similar solvent-dependent photoluminescence behavior has been reported in luminescent metal–organic frameworks (MOFs) where hydrogen bonding in polar protic solvents enhanced emission intensity (X. Zhao & Yang, 2020). This observation supports the use of methanol as the preferred sensing medium for Complex 1.

The photoluminescence intensity of Complex 1 varied significantly across solvents, as shown in Figure 4.10. Methanol recorded the highest intensity (783.4 units), followed by n-hexane (121.3 units), 1,4-dioxane (60.7 units), and acetonitrile (28.1 units), while distilled water produced the lowest intensity (15.6 units).

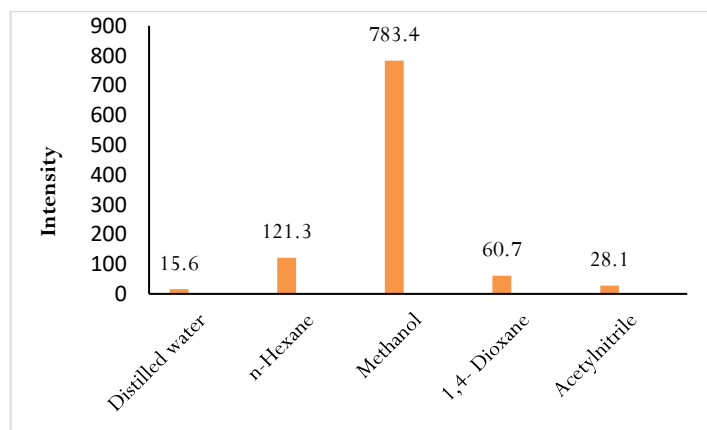


Figure 12. Graph showing different intensities of complex 1 in different solvents

The exceptional response in methanol likely results from enhanced solvation and optimal dispersion, whereas the reduced intensity in water can be linked to aggregation and fluorescence quenching due to hydrogen-bonded water networks. Similar

effects have been noted by (Besford et al., 2022), who observed that polar aprotic solvents such as ACN generally produce lower luminescence in MOF systems due to competitive coordination with metal centers, disrupting the emissive pathway.

3.8 Analyte Specificity

A methanolic suspension of Complex 1 (1 mg in 5 mL methanol; Suspension 1) was used to test selectivity toward nitroaromatic explosives. Separate 10 mM solutions of picric acid (PA), 4-nitroaniline (4-NA), 4-nitrophenol (4-NP), and 4-nitrotoluene (4-NT) were prepared, and 30 μL of each was added to Suspension 1.

The quenching efficiencies were calculated using formula:

$$I_0 - I \div I_0$$

where I_0 is the fluorescence intensity before the addition of the analyte, and I is the intensity after addition.

The results showed picric acid with the highest quenching efficiency (92.20%), followed by 4-NT (43.10%), 4-NA (10.40%), and 4-NP (5.70%). The markedly higher quenching by picric acid is attributed to its strong electron-withdrawing –NO₂ groups, facilitating efficient photoinduced electron transfer (PET) from the excited ligand to the analyte. Such selectivity toward picric acid is consistent with previous MOF-based sensors where strong π – π interactions and electron-deficient aromatic rings promoted higher quenching efficiency (Pal, 2022).

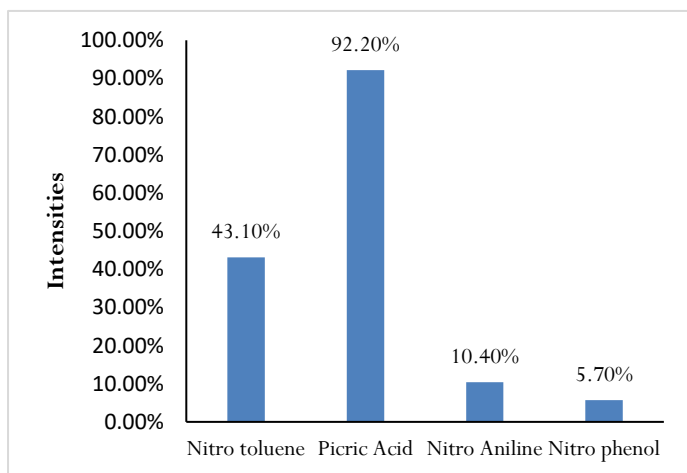


Figure 13. Graph shows the quenching efficiencies of different nitro aromatic compounds.

Further titration with increasing picric acid concentrations (0–5 mM) demonstrated a gradual decrease in emission until complete quenching at 1 mM. The photoluminescence (PL) intensity of Complex 1 in methanol upon the gradual addition of a 1 mM solution of picric acid. A complete quenching of fluorescence was

observed, indicating 100% quenching efficiency. The quenching efficiency (%Q) was calculated using the formula:

$$\%Q = (I_0 - I) / I_0 \times 100,$$

where I_0 represents the fluorescence intensity of the complex before the addition of the analyte, and I is the intensity after the addition.

To further evaluate the sensing behavior, a linear analysis was the fluorescence quenching response of the complex increases progressively with the rising concentration of picric acid from 0.2 mM to 1.0 mM. The ratio I_0/I (fluorescence intensity before and after analyte addition) shows a near-linear relationship in the initial concentration range, consistent with the Stern–Volmer equation:

$$I_0/I = 1 + K_{sv} \times [PA],$$

where I_0/I is the ratio of fluorescence intensities before and after picric acid addition, K_{sv} is the Stern–Volmer quenching constant, and $[PA]$ is the molar concentration of picric acid. The fitted linear regression equation, $y=1.2269x-0.4065$ with a correlation coefficient $R^2=0.8518$ indicates a reasonably strong linear dependence between quenching efficiency and picric acid concentration. This suggests that the quenching mechanism is predominantly dynamic in nature at lower analyte concentrations.

At higher concentrations (above 0.8 mM), the deviation from ideal linearity becomes more pronounced, which could be attributed to factors such as static quenching, complex formation, or partial saturation of active sites on the complex. The observed increase in quenching efficiency confirms strong interactions between the complex and picric acid, likely driven by electron transfer processes from the ligand to the nitroaromatic analyte.

Complex 2:

Selectivity of the solvent:

For solvent selection, 1 mg of Complex 2 was dispersed in different solvents, including methanol, 1,4-dioxane, distilled water, acetonitrile (ACN), and n-hexane. Partial solubility was observed in all solvents, and each dispersion was stabilized by 10 minutes of bath sonication. The fluorescence spectra were then recorded to evaluate solvent influence on emission behavior. The results (Figure 4.18 supplementary file) clearly indicate methanol as the optimal medium, exhibiting the highest fluorescence emission intensity, followed by 1,4-dioxane. Distilled water produced the lowest intensity, while ACN and n-hexane also showed minimal luminescence. When excited at 310.00 nm in methanol, Complex 2 displayed a strong emission peak at

730.424 nm, suggesting high compatibility with polar protic environments.

This solvent dependence is consistent with reports by (Terrón et al., 2025), who found that protic solvents like methanol can enhance photoluminescence in MOFs by promoting hydrogen bonding and stabilizing excited states, whereas nonpolar or competitive-coordination solvents reduce emission through non-radiative decay or quenching effects.

3.9 Intensities of Different Solvents

Photoluminescence of Suspension 2 based on Complex 2 dependence of the solvent was characterized across several solvents such as distilled water, acetonitrile, methanol, 1,4-dioxane and n-hexane. The emission intensity was highly dependent on the solvent surrounding as demonstrated in Figure 14 indicating strong solvent selectivity. Methanol gave the largest emission intensity of such fluorophore (~720 units), meaning an enhanced solubility and a stable dispersion since it is a polar protic solvent with the capacity to form hydrogen bonds. In comparison, the intensity of 1,4-dioxane was moderate (~140 units), indicating less, but good interaction.

Conversely, very poor solubility and insignificant interactions were evidenced by acetonitrile and n-hexane as they showed very low emission. Acetonitrile even showed a slightly negative intensity, likely due to baseline correction or quenching effects. Distilled water also produced minimal fluorescence, possibly due to aggregation or limited compatibility with the complex.

These observations confirm that methanol provides the most suitable environment for maximizing the luminescence of Complex 2, making it ideal for further sensing applications.

3.10 Analyte specificity:

To evaluate analyte specificity, a methanolic suspension of Complex 2 (1 mg in 5 mL methanol; Suspension 2) was prepared, and 10 mM solutions of four nitroaromatic compounds picric acid (PA), 4-nitroaniline (4-NA), 4-nitrophenol (4-NP), and 4-nitrotoluene (4-NT) were tested. In each case, 30 μ L of the analyte solution was added to the suspension, and quenching efficiency was calculated using.

$(I_0 - I) / I_0$

As shown in figures 4.20–4.24, picric acid exhibited the highest quenching efficiency at 89.8%, followed by 4-nitroaniline (30.61%), 4-nitrophenol (16.3%), and 4-nitrotoluene (7.80%). The strong selectivity toward picric acid can be attributed to its multiple nitro groups and strong electron-withdrawing nature,

which facilitate efficient electron transfer from the photoexcited ligand of Complex 2 to the analyte. This behavior is consistent with previous findings in luminescent MOFs, where electron-deficient nitroaromatics, especially picric acid, act as strong quenchers via a photoinduced electron transfer (PET) mechanism (Xu et al., 2019)

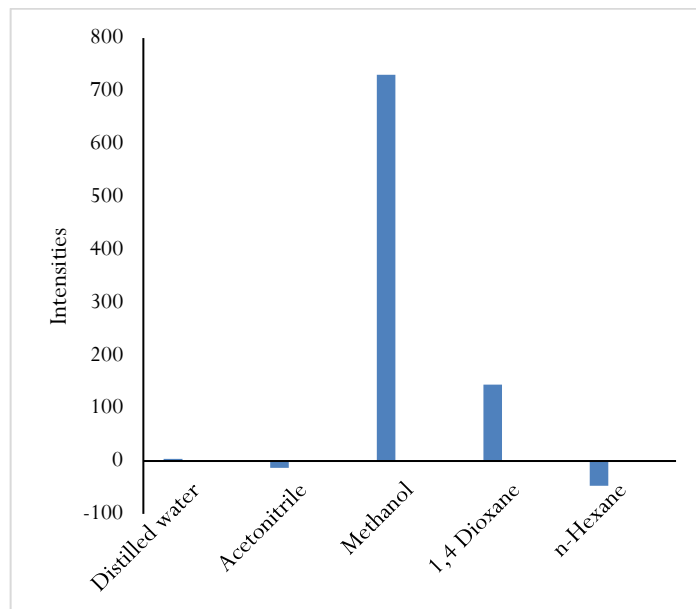


Figure 14. Graph showing different intensities of complex 2 in different solvents

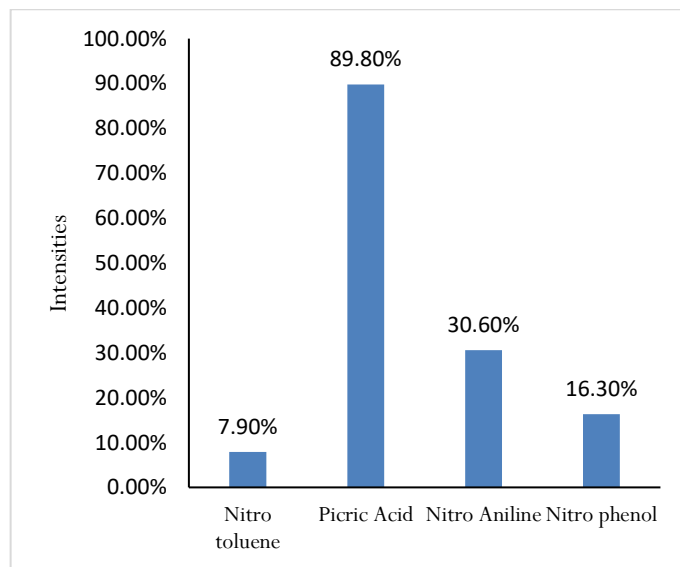


Figure 15. Graph shows the quenching efficiency of suspension 2 in different nitro aromatic compounds

Specificity of the analyte was chosen by comparing the fluorescence intensity of different analytes in the suspension of

complex 2 in methanol. 10mM concentration of different nitro compounds was prepared and was added in suspension 2 and then compared to the fluorescent intensities by using formula

I_0 = intensity of the complex before the addition of analyte

I = intensity of the complex after the addition of analyte

$I_0 - I \div I_0$

It was concluded that complex 2 is specific for picric acid because it quenches significantly. The emission intensity depends on the nature of analyte because of electron transfer between complex and analyte. Finally, it was noticed that this complex 2 could quench picric acid 100% (% quenching efficiency), that was calculated by

$$\%Q = (I_0 - I/I_0)$$

I_0 = Intensity of complex before addition of analyte

I = Intensity of complex after addition of analyte

For linear analysis, the suspension of 2 in Methanol was run through linear fitting analysis. 0- 5mM concentration of Picric acid was made and then fluorescence quenching was observed. The data obtained was well fitted in the linear equation.

$$y = 1.2269x + 0.357 (R^2 = 0.9966)$$

It was observed that at the lower concentration good linearity obtained which is accordance to the Stern- Volmer equation.

According to the Stern-Volmer equation:

$$I_0/I = 1 + K_{sv} \times [Pa]$$

Here I_0/I is the fluorescence intensities of complex 2 in Methanol suspension before and after the addition of different concentrations of Picric acid in it. K_{sv} is the stern binding constant and Pa is the molar concentration of Picric Acid. The calculated Stern–Volmer constant (K_{sv}) for Complex 2 with picric acid was 2.087 mM^{-1} , indicating a stronger binding interaction compared to Complex 1, possibly due to differences in pore structure or electronic configuration.

3.11 Comparative Performance of Complex 1 and Complex 2

While both complexes exhibited strong selectivity and sensitivity toward picric acid, the presence of PDA in Complex 2 appears to slightly improve quenching efficiency and K_{sv} values, potentially due to enhanced hydrogen bonding and π -electron interactions. The solvent-dependent behavior was consistent across both complexes, with methanol providing optimal dispersion and maximum emission intensity. This study confirms that Ce–BTCA and Ce–BTCA–PDA frameworks are promising

candidates for luminescent explosive sensing applications, particularly for picric acid detection. The combination of rapid sonochemical synthesis, strong photoluminescence, and high selectivity makes these materials viable for potential use in real-time sensing devices for security and environmental monitoring.

The luminescent sensing performance of the synthesized cerium-based metal–organic complexes demonstrate their strong potential for selective detection of nitroaromatic explosives, particularly picric acid. Both complexes exhibited solvent-dependent photoluminescence behavior, with methanol identified as the most suitable medium due to enhanced solvation, improved dispersion, and suppression of non-radiative decay pathways. This observation aligns with previous reports where polar protic solvents enhanced emission efficiency in luminescent coordination polymers and MOFs [2,14].

The selective quenching response toward picric acid compared to other nitroaromatic compounds such as 4-nitroaniline, 4-nitrophenol, and 4-nitrotoluene can be attributed to the strong electron-withdrawing nature of the multiple nitro groups present in picric acid. These functional groups facilitate efficient photoinduced electron transfer (PET) from the excited ligand framework to the analyte, resulting in significant fluorescence quenching [4,7]. Additionally, π - π stacking interactions and hydrogen bonding between picric acid and the ligand framework further enhance analyte–sensor interactions.

Comparative analysis of the two complexes revealed that the incorporation of the co-ligand in Complex 2 significantly improved sensing performance, as evidenced by higher quenching efficiency and larger Stern–Volmer constants. This enhancement may be associated with increased hydrogen bonding sites and modified electronic environments introduced by the co-ligand, which promote stronger interactions with picric acid molecules [10,13]. The near-linear Stern–Volmer relationship observed at lower analyte concentrations suggests a predominantly dynamic quenching mechanism, while deviations at higher concentrations may indicate contributions from static quenching or site saturation effects.

Overall, the results confirm that Ce–BTCA and Ce–BTCA–PDA complexes function as efficient luminescent probes for nitroaromatic explosive detection. Their rapid response, high selectivity, and sensitivity make them promising candidates for practical applications in forensic investigations, security screening, and environmental monitoring. Compared to conventional analytical techniques, these luminescent sensors

offer advantages such as operational simplicity, rapid detection, and cost-effectiveness, supporting their potential integration into portable explosive detection platforms.

4. Conclusion

In this study, two cerium-based metal–organic complexes were successfully synthesized using the sonication method, employing the same cerium metal center but different ligand compositions cerium–1,2,4,5-benzenetetracarboxylic acid and cerium–1,2,4,5-benzenetetracarboxylic acid–2-[(hydroxyl-2-methyl-5-phosphonoxymethyl-pyridine-4-ylmethyl)-amino]-propionic acid. Both complexes were fully characterized using Fourier-transform infrared spectroscopy to confirm the coordination of functional groups, ultraviolet–visible spectroscopy to verify the binding of the cerium metal with the ligand, and photoluminescence spectroscopy to evaluate their optical properties and sensing capability. Fluorescence sensing experiments showed that both complexes possess high selectivity and sensitivity toward picric acid (2,4,6-trinitrophenol) in the

solution phase, while exhibiting considerably lower responses toward other nitroaromatic analytes such as 4-nitroaniline, 4-nitrophenol, and 4-nitrotoluene. The first complex demonstrated solvent-dependent luminescence, with methanol producing the highest fluorescence intensity. The second complex, incorporating the co-ligand 2-[(hydroxyl-2-methyl-5-phosphonoxymethyl-pyridine-4-ylmethyl)-amino]-propionic acid, exhibited enhanced recognition of picric acid and higher Stern–Volmer constants. In conclusion, cerium metal complexes synthesized with 1,2,4,5-benzenetetracarboxylic acid, particularly when functionalized with an appropriate co-ligand, are ideal luminescent markers for the selective and sensitive detection of explosive nitroaromatic compounds. Their ability to rapidly and reliably detect trace quantities of explosives makes them highly significant for forensic science applications, where precise, sensitive, and timely explosive analysis is critical for criminal investigations, counter-terrorism measures, and public safety

Funding: No Funding is avail for this research

Data Availability Statement: The data supporting the findings of this study are available in the Lab manual at Institute of Molecular Biology and Biotechnology, Department of Forensic Science, The University of Lahore, Lahore, Pakistan.

Acknowledgments: We acknowledge Institute of Molecular Biology and Biotechnology, Department of Forensic Science, The University of Lahore, Lahore, Pakistan for facilitating and providing chemicals, lab access, resources and his administrative support throughout this project.

Conflicts of Interest: Authors declare there is no conflict of interest.

References

1. Abdi MR, Sarlak N. Magnetic metal–organic frameworks for determination of heavy metals in different cosmetic products available in Iran market by flame atomic absorption spectroscopy. *Anal Bioanal Chem Res.* 2025;12(1):11–25. doi:10.22036/abcr.2024.457668.2108.
2. Besford QA, Van den Heuvel W, Christofferson AJ. Dipolar dispersion forces in water–methanol mixtures: enhancement of water interactions upon dilution drives self-association. *J Phys Chem B.* 2022;126(33):6231–6239. doi:10.1021/acs.jpcc.2c04638.
3. Chen J, Cheng F, Luo D, Huang J, Ouyang J, Nezamzadeh-Ejchieh A, et al. Recent advances in Ti-based MOFs in biomedical applications. *Dalton Trans.* 2022;51(39):14817–14832. doi:10.1039/D2DT02470E.
4. Cui H, Liu W, Xu X, Zhou J, Song X, Chen X. Synthesis and fluorescence sensing for nitro explosives and pesticides of two Cd-coordination polymers. *ACS Omega.* 2023;8(42):39917–39927. doi:10.1021/acsomega.3c06439.
5. Ding L, Yu ZD, Wang XY, Yao ZF, Lu Y, Yang CY, et al. Polymer semiconductors: synthesis, processing, and applications. *Chem Rev.* 2023;123(12):7421–7497. doi:10.1021/acs.chemrev.2c00696.
6. Guo J, Xue X, Yu H, Duan Y, Li F, Lian Y, et al. Metal–organic frameworks based on infinite secondary building units: recent progress and future outlooks. *J Mater Chem A.* 2022;10(37):19320–19347. doi:10.1039/D2TA03159K.
7. Pal TK. Metal–organic framework (MOF)-based fluorescence “turn-on” sensors. *Mater Chem Front.* 2022;7(3):405–441. doi:10.1039/D2QM01070D.

8. Roy M, Sengupta S, Bala S, Bhattacharya S, Mondal R. Systematic study of mutually inclusive influences of temperature and substitution on the coordination geometry of Co(II) in a series of coordination polymers and their properties. *Cryst Growth Des.* 2016;16(6):3170–3179. doi:10.1021/acs.cgd.5b01835.
9. Socha BN, Patankar B, Raj A, Palan RB, Valand J, Patel RH, et al. Efficient green one-pot MOF synthesis for ultra-fast wastewater treatment and industrial catalytic applications. *Chem Eng J.* 2024;493:152566. doi:10.1016/j.ccej.2024.152566.
10. Sun L, Zhang Y, Lv X, Li H. A luminescent Eu-based MOF material for the sensitive detection of nitro explosives and fingerprint development. *Inorg Chem Commun.* 2023;156:111267. doi:10.1016/j.inoche.2023.111267.
11. Terrón D, Sanromán A, Pazos M. Metal–organic frameworks: next-generation materials for environmental remediation. *Catalysts.* 2025;15(3). doi:10.3390/catal15030244.
12. Wang J, Chen NN, Zhang C, Jia LY, Fan L. Functional group-induced structural diversities and photocatalytic, magnetic, and luminescence sensing properties of four cobalt(II) coordination polymers. *CrystEngComm.* 2020;22(4):811–820. doi:10.1039/C9CE01474H.
13. Zhao D, Yu S, Jiang WJ, Cai ZH, Li DL, Liu YL, et al. Recent progress in metal–organic framework-based fluorescent sensors for hazardous materials detection. *Molecules.* 2022;27(7). doi:10.3390/molecules27072226.
14. Zhao X, Yang S. Photoinduced excited-state hydrogen bonding strengthening of hemiindigo for drastically fluorescence quenching in protic solvent and water sensing in aprotic solvent. *J Lumin.* 2020;220:116993. doi:10.1016/j.jlumin.2019.116993.
15. Zhou M, Frenking G. Transition-metal chemistry of the heavier alkaline earth atoms Ca, Sr, and Ba. *Acc Chem Res.* 2021;54(15):3071–3082. doi:10.1021/acs.accounts.1c00277.